

# Current Biology

## Gamma Power Reductions Accompany Stimulus-Specific Representations of Dynamic Events

### Highlights

- Dynamic stimulus-specific representations can be tracked in iEEG gamma activity
- Stimulus-specific gamma activity reoccurs specifically during successful retrieval
- Global (brain-wide) and local (electrode-wise) representations match
- Global and local gamma power reductions accompany more reliable representations

### Authors

Hui Zhang, Juergen Fell, ...,  
Christian E. Elger, Nikolai Axmacher

### Correspondence

nikolai.axmacher@rub.de

### In Brief

Zhang et al. find that human intracranial electroencephalogram patterns are sensitive to the content of virtual navigation sequences and reoccur if participants remember them. More reliable representations are related to reductions of neural activity at high (gamma) frequency. The findings shed new light on the neural basis of content-specific representations.

# Gamma Power Reductions Accompany Stimulus-Specific Representations of Dynamic Events

Hui Zhang,<sup>1</sup> Juergen Fell,<sup>2</sup> Bernhard P. Staresina,<sup>3</sup>  
Bernd Weber,<sup>2,4,5</sup> Christian E. Elger,<sup>2</sup>  
and Nikolai Axmacher<sup>1,6,\*</sup>

<sup>1</sup>Department of Neuropsychology, Institute of Cognitive Neuroscience, Ruhr-University Bochum, 44801 Bochum, Germany

<sup>2</sup>Department of Epileptology, University of Bonn, 53105 Bonn, Germany

<sup>3</sup>School of Psychology, University of Birmingham, Birmingham B15 2TT, UK

<sup>4</sup>Center for Economics and Neuroscience, 53127 Bonn, Germany

<sup>5</sup>Life and Brain Center, University of Bonn, 53127 Bonn, Germany

<sup>6</sup>German Center for Neurodegenerative Diseases (DZNE), 53175 Bonn, Germany

## Summary

Neural representations of specific stimuli rely on activity patterns in distributed neural assemblies [1–4]. According to one influential view, these assemblies are characterized by synchronized gamma-band activity (GBA) [5–11] that reflects stimulus-specific representations [12–14]. However, recent studies have shown that GBA is closely correlated with the overall amount of cellular activity and may be detrimental for precise representations of specific stimuli [15, 16]. Until now, the role of GBA for the formation of dynamically changing representations has been unknown. Here, we applied representational similarity analysis (RSA) [17] to intracranial electroencephalogram (iEEG) data from ten presurgical epilepsy patients to identify stimulus-specific neural representations. Patients first learned and then retrieved their paths through virtual houses. Dynamic representations were identified by the rapidly changing distributions of frequency-specific global (spatial) activity patterns across the brain. We found that GBA patterns during successful (but not unsuccessful) retrieval of one sequence were more similar to activity during encoding of that same sequence compared to other sequences. The contribution of individual electrodes to these global representations was correlated with local similarity in individual electrodes (i.e., with RSA across time). Moreover, time-resolved RSA values were negatively correlated with the magnitude of iEEG gamma power: RSA values were higher at time points when gamma power was reduced. Both global and local representations relied on a small proportion of electrodes. These results show that behaviorally relevant neural representations of specific dynamically changing stimuli can be tracked by iEEG recordings and that they are associated with reductions of gamma power.

## Results

Patients were presented with video sequences showing the first person perspective of navigating through a furnished

virtual house (Figures 1A and 1B; Supplemental Information 2.1–2.3). The same dynamic sequences were displayed during one encoding and three consecutive retrieval sessions. We quantified the reliability of neural representations by calculating the similarity between encoding and retrieval of dynamic episodes using representational similarity analysis (RSA) [17]. We applied both global (spatial) and local (temporal) RSA to examine global and local representational similarity in intracranial electroencephalogram (iEEG) data. Global representational similarity was analyzed by calculating correlations across electrodes, yielding a time-frequency-resolved metric of global (brain-wide) stimulus-specific representations. Local representational similarity was quantified via correlations across time courses, resulting in local representations in individual electrodes. For simplicity, in the following RSA refers to global RSA unless otherwise specified.

## Global Representational Similarity Is Higher between Encoding and Successful Retrieval of Same Video Sequences Compared with Different Ones

One of our main goals was to assess whether retrieval of a dynamic episode was associated with the same global neural activity patterns that had occurred during encoding of that episode. Two examples of this analysis are shown in Figures 2A<sub>i</sub> and 2A<sub>ii</sub>, taken from two different trials in two different patients. Each of these figures indicates the distribution of EEG power at one specific time point and at one specific frequency. These distributions were then compared (using Spearman's rank statistics) between encoding and retrieval of the same perceptual input. We thus analyzed the similarity of neural activation patterns across the brain between encoding and retrieval. We calculated encoding-retrieval correlations across electrodes in various time-frequency bins within each patient (see examples in Figure 2B) and then performed cluster-based surrogate statistics across the group of patients (Supplemental Information 2.4; Figure S1). This method effectively controls the alpha level for multiple comparisons on an assumption-free basis regarding the sampling distribution under the null hypothesis. We found significant clusters mainly in the high-frequency range prior to the decision point at a (corrected) alpha level of  $p < 0.001$  (Figures 2C–2D). More specifically, when we fitted a Gaussian function to the distribution of significant time bins (right part of Figure 2D), this function showed a peak at a frequency of 81 Hz and an SD of 39 Hz. Therefore, we selected a frequency range between 42 and 120 Hz for the following analyses (mean  $\pm$  1 SD). This result indicates that gamma-band activity (GBA) during retrieval of a dynamic sequence resembles activity during encoding of that same sequence more than activity during encoding of a different sequence.

The amount of similarity was behaviorally relevant, because the same analysis for incorrectly retrieved trials did not yield any significant clusters ( $p_{corr} = 0.979$ ; i.e., the summary  $t$  value of the largest cluster for incorrect trials was smaller than 97.9% of the summary  $t$  values of surrogate clusters; Figure 2D<sub>ii</sub>). This lack of an effect was not due to the smaller number of incorrect trials (accuracy of three retrieval sessions: 78.6%, 85.3%, and 90.6%; Figure 1C; Supplemental Information 3.1) because

\*Correspondence: [nikolai.axmacher@rub.de](mailto:nikolai.axmacher@rub.de)

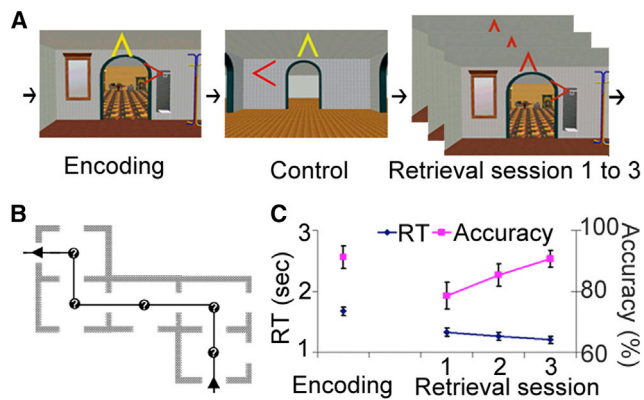


Figure 1. Paradigm and Behavioral Results

(A) Experimental procedure involving encoding, control (distraction), and retrieval of a video sequence of navigating through a virtual house. (B) Schematic overview of the path through one house. The black line with arrows indicates the navigation path inside the house. The question marks were decision points when arrows were displayed and patients had to remember the correct path. (C) Behavioral results: response accuracy and reaction times during encoding and three retrieval sessions. Error bars indicate 1 SEM.

results for successful trials remained very similar when we randomly selected as many successful trials as there were unsuccessful trials (Figure S2A). Furthermore, the summary  $t$  value of the largest cluster of incorrect trials was smaller than 93.13% of the summary  $t$  values of all clusters found for this reduced subset of correct trials (see Supplemental Information 2.4). We also conducted additional analyses to rule out possible confounds of temporal proximity, perceptual similarity, and re-encoding during retrieval (Figures S2B–S2H; Supplemental Information 3.2–3.4).

### Topographical Distributions of Stimulus-Specific Representations Are Sparse and Correlated with Local RSA

We evaluated the contribution of individual electrodes to global stimulus-specific representations for both correct and incorrect trials. To this end, we performed a jackknife procedure and calculated changes in RSA values after leaving out individual electrodes (Supplemental Information 2.5). Interestingly, only 29.2% of all electrodes (57/195; “informative” electrodes) showed positive contributions to RSA values of correct trials (Figure 3A); in other words, activity in 70.8% of all electrodes (138/195; “non-informative” electrodes) was detrimental to neural representations. There were more electrodes that showed positive contributions to RSA values of incorrect trials (40.5%, i.e., 79/195) compared with correct trials ( $\chi^2(1) = 12, p < 0.001$ ). Informative electrodes were mainly located in higher visual areas (Figure S3A; Supplemental Information 3.5).

In the analyses presented thus far, we focused on global representations across the brain, by analyzing the similarity of activity patterns across the spatial dimension (i.e., across electrodes). On the other hand, individual brain regions may support representations of a specific sequence as well. To investigate this question, we calculated local RSA values across time separately in each individual electrode (Figures 3B, 3C, and S3B; Supplemental Information 2.5 and 3.6). These local RSA values were significantly correlated with the contribution of individual electrodes to global representations

( $r = 0.357, p < 0.001$ ; Figure 3D), indicating that local and global representations are related to each other. In contrast to correct trials, local RSA values in incorrect trials were independent of their contribution to global representations ( $r = -0.04, p = 0.59$ ; Figure 3D<sub>ii</sub>).

### Dynamic Stimulus-Specific Global Representations Are Associated with Gamma Power Reductions

The results presented thus far show that dynamic sequences of specific stimuli are represented by dynamically changing patterns of GBA. Next, we assessed whether these distributed representations depend on overall GBA magnitude during retrieval (averaged across electrodes), i.e., whether higher or lower levels of brain-wide GBA during retrieval (when representations should be reactivated) are related to more reliable representations. We found that the time courses of RSA values were negatively correlated with the time courses of GBA during retrieval (Figure 4A). This relationship was specific for correct trials ( $t(9) = -3.82, p = 0.004$ ) and did not occur for incorrect trials ( $t(9) = -0.45, p = 0.65$ ). Similar results were obtained when only the informative electrodes were taken into account (correct trials:  $t(9) = -3.19, p = 0.01$ ; incorrect trials:  $t(9) = 1.56, p = 0.15$ ). A direct comparison showed that the correlation of RSA values and GBA was more negative for correct than for incorrect trials ( $t(9) = -3.17, p = 0.01$ ), which was also true for the subset of informative electrodes ( $t(9) = -3.28, p = 0.0096$ ). These results show that more reliable representations of specific dynamic stimuli are associated with reductions of global EEG power. Further analyses showed that these findings are specific to the gamma frequency range (Supplemental Information 3.7).

Next, we analyzed whether the magnitude of GBA in individual electrodes is related to the reliability of distributed representations. Therefore, we correlated, for each electrode and each trial, GBA during retrieval with the time courses of global RSA values in the gamma frequency range. A one-sample  $t$  test was then applied to Fisher’s  $z$ -transformed correlation values across trials. This analysis revealed for correct trials that (after Bonferroni correction) 24.6% of all electrodes (48/195) showed significantly negative correlations (Figures 4B and S4A; Supplemental Information 3.8). Only 2 of 195 electrodes, which were both located in the hippocampus of one single patient, showed significant positive correlations between gamma power and RSA values in the gamma band. Moreover, informative electrodes showed significant negative GBA-RSA correlations ( $t(56) = -5.53, p < 0.001$ ), which were significantly more negative than in non-informative electrodes ( $t(193) = -2.56, p = 0.01$ ; Figure S4B). Higher RSA values for informative than non-informative electrodes were also found when we separately averaged temporal RSA values for the two groups of electrodes in each patient (paired  $t$  test across patients:  $t(9) = 2.95, p = 0.02$ ; Figure 4C). For incorrect trials, only a single electrode (located in the hippocampus) showed a significantly negative correlation, and no electrode showed a positive correlation.

These results suggest that higher levels of GBA are detrimental for the reliability of neural representations. To further validate this interpretation, we first focused only on informative electrodes. Temporal RSA values were averaged across trials with highest gamma power (top one-third) and lowest gamma power (bottom one-third) within each electrode. A paired  $t$  test across electrodes showed that temporal RSA values were larger for trials with the lowest gamma power compared to trials with the highest gamma power

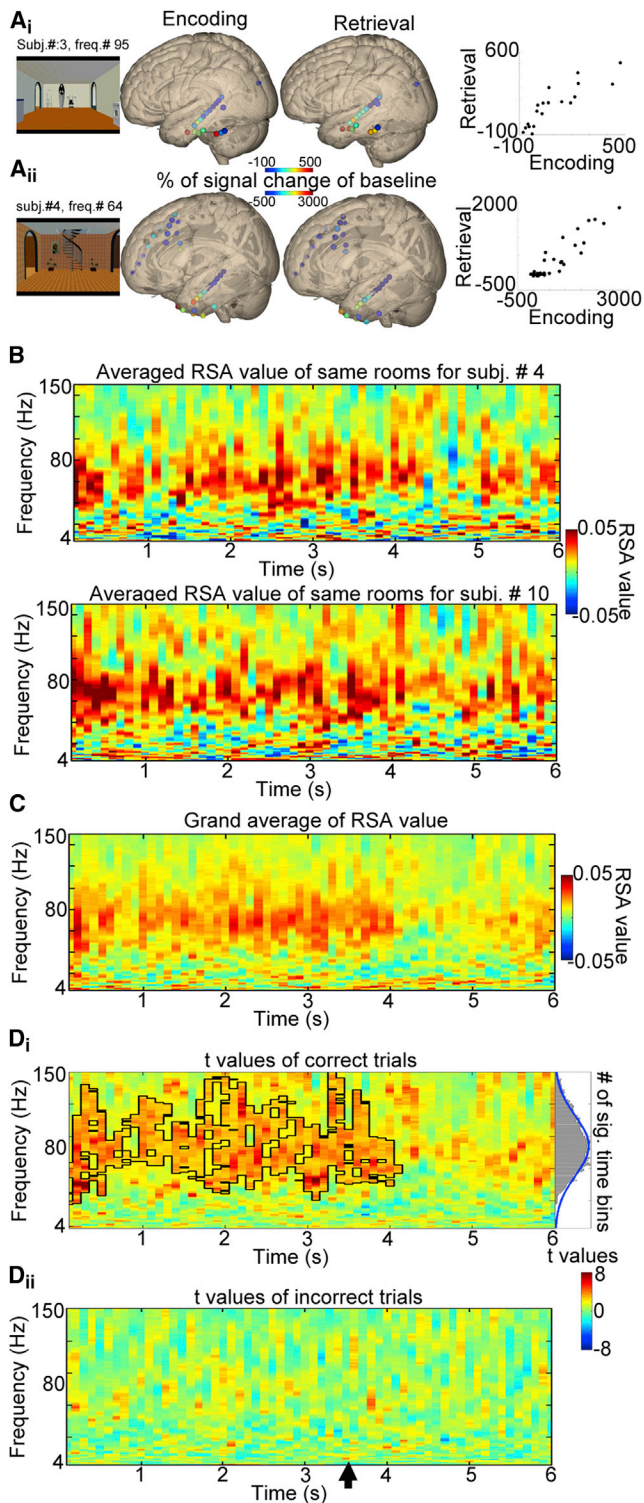


Figure 2. Spatial Representational Similarity Analysis

(A<sub>i</sub> and A<sub>ii</sub>) Two single-trial examples (A<sub>i</sub> and A<sub>ii</sub>) of topographical patterns of GBA across the brain during encoding and retrieval of identical positions within a virtual house. Left: position in virtual houses during encoding and retrieval (top: position during encoding and retrieval in example 1; bottom: position during encoding and retrieval in example 2). Middle: each colorful sphere in the transparent brain indicates an electrode, with colors representing the magnitude of GBA (42–120 Hz) at the respective time points. Right: scatter plot of the same results (each dot indicates one electrode) as indicated in the middle panel.

( $t(56) = -2.78, p = 0.007$ ; Figure 4D). By contrast, we did not find such an effect in the non-informative electrodes ( $t(137) = -0.84, p = 0.40$ ). We also compared the magnitude of gamma power during successful compared to unsuccessful retrieval. Indeed, we found that gamma power was higher when participants were unable to successfully remember a path compared to successful retrieval trials ( $t(194) = -8.37, p < 0.001$ ; Figures 4E and S4C; if only informative electrodes were included,  $t(56) = -4.36, p < 0.001$ ). In general, gamma power was lower during retrieval compared to encoding (Supplemental Information 3.9; Figure S4D), and the magnitude of this reduction was correlated with faster reaction times ( $t(9) = 2.74, p = 0.02$ ). By contrast, we did not find any significant difference of the gamma power between encoding and retrieval for incorrect trials.

## Discussion

### Reinstatement of Dynamic Stimulus-Specific Representations during Memory Retrieval

A long-standing hypothesis in memory research is that memory retrieval consists in the reinstatement of encoding-related activity patterns [18]. Several recent studies have investigated the similarity between neural activity during encoding and retrieval of specific events [19]. In fMRI data, pattern classification analyses [20, 21] and RSA [22–24] have shown significant similarity between encoding and retrieval of specific events. Similar results have been obtained in iEEG studies based on RSA [13] and on sequences of single units [25]. Our data presented here are consistent with the general finding that neural activity during successful retrieval of an event resembles activity during encoding of that event. While most previous studies on encoding-retrieval similarity of stimulus-specific representations have used static stimuli such as words or objects, in some of them movie sequences were presented [25–27]. Such dynamic stimuli are more ecologically valid than static ones [28]; however, to our knowledge, very few studies [29–31] have investigated the temporal dynamics of neural similarity patterns for repeated dynamic stimuli and their functional role for memory processes.

### Relationship between RSA Values and GBA

Overall, we found that time periods during which RSA values were high were associated with reductions of EEG power in the gamma frequency range, both when averaged across the brain and when individually considered in single electrodes. In the iEEG, GBA shows spatial correlations just in the millimeter domain [32, 33] and thus corresponds to activity of relatively circumscribed neural networks. Several studies have shown that GBA in a narrow frequency band reflects the recruitment of neural assemblies that are phase synchronized at this frequency [5, 34–37]. On the other hand, some recent

(B) Examples of averaged RSA values across correct trials for two subjects. (C) Grand average of RSA values of correct trials.

(D<sub>i</sub> and D<sub>ii</sub>) Statistical results of the comparison of RSA values during encoding and retrieval of the same episode compared to encoding and retrieval of different electrodes, cluster corrected for multiple comparisons. Significant clusters are circled by black lines. Statistical results are presented for correct (D<sub>i</sub>) and incorrect (D<sub>ii</sub>) trials. Right panel of D<sub>i</sub>: distribution of significant RSA time bins across frequencies with fitted Gaussian function (blue line). Arrow indicates time points when arrow display started. In (B) to (D), time 0 indicates the time point when participants start navigating into a new room.

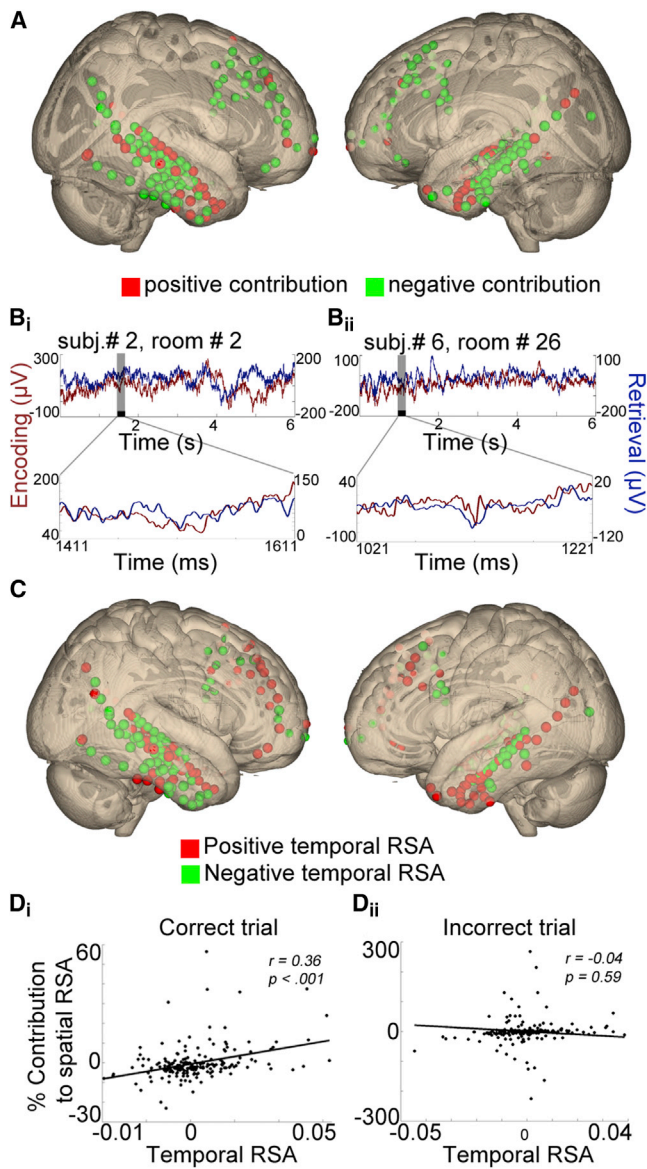


Figure 3. Spatial and Temporal Representations

(A) Positive (red) and negative (green) contribution of individual electrodes to spatial RSA (i.e., RSA across electrodes, as depicted in Figure 2) as assessed by a jackknife procedure.

(B<sub>i</sub> and B<sub>ii</sub>) Two examples (B<sub>i</sub> and B<sub>ii</sub>) of raw data for calculating local RSA (i.e., RSA calculated across time for individual electrodes). Data show single-trial examples for two episodes when two patients were navigating through the same virtual room during encoding (dark red) and retrieval (blue) across the entire time interval of 6 s (top panel) and within a smaller time window of 200 ms (bottom panel)

(C) Local (temporal) representations across the brain. Red indicates positive temporal RSA values, and green indicates negative temporal RSA values in individual electrodes.

(D<sub>i</sub> and D<sub>ii</sub>) Correlation between the contribution of each electrode to global (spatial) RSA and local (temporal) RSA values for both correct (D<sub>i</sub>) and incorrect trials (D<sub>ii</sub>). Each dot indicates one electrode.

studies showed that the broadband changes in GBA, which are often observed in iEEG studies (for a recent study, see [38]), correlate with the magnitude of multi-unit activity [39, 40] and may thus rather reflect the overall amount of cellular excitation than the degree of neural synchronization. The

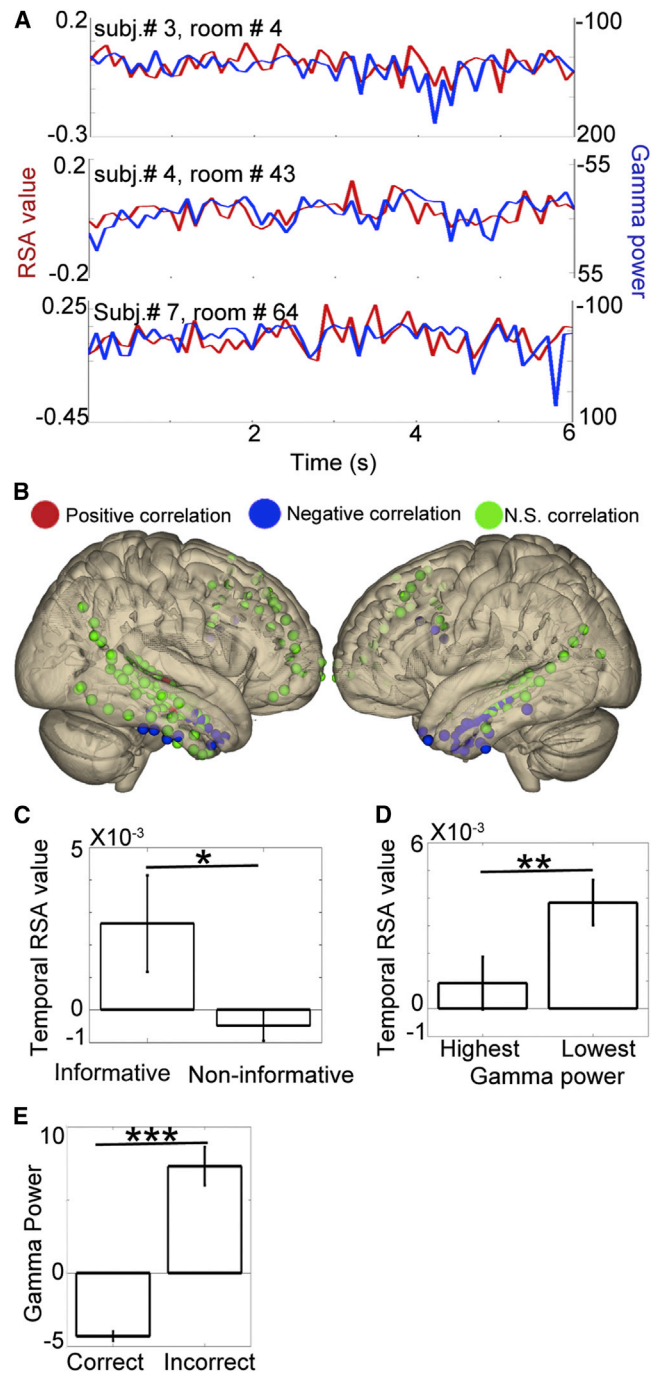


Figure 4. High Representational Reliability Is Related to Reductions of EEG Gamma Power of Correct Trials

(A) Three single-trial examples of raw RSA values (red) and gamma power time series (blue). Unit of gamma power: percentage of signal change compared to baseline. For presentation purposes, we plotted the data at a reduced sampling rate of 10 Hz.

(B) Distribution of electrodes showing significantly negative (blue) and positive (red) correlations between RSA values and EEG power in the gamma band. (C) Averaged temporal RSA value in informative and non-informative electrodes. Error bars indicate 1 SEM.

(D) Averaged temporal RSA value of trials with highest and lowest third of gamma power in informative electrodes. Error bars indicate 1 SEM.

(E) Average gamma power during correct and incorrect retrieval trials. Error bars indicate 1 SEM. Unit of gamma power is percentage of signal change to baseline. In (C)–(E), a significant difference between two groups is indicated with \* $p < 0.05$ , \*\* $p < 0.01$ , and \*\*\* $p < 0.001$ .

relative contribution of excitation and synchronization to GBA is currently unclear. Most likely, synchronization-related (narrow-band) GBA and activity-related (broadband) GBA coexist [41]. The situation becomes even more complex because gamma band synchronization, on the one hand, crucially relies on the activity of inhibitory interneurons [42] and is thus related to inhibition, but enhances, on the other hand, the efficiency with which synchronized neurons activate their target structures (coincidence detection) [43, 44], relating GBA to excitation.

Our results presented here speak against theories that high levels of GBA reflect synchronized neural assemblies that represent specific events [6, 7, 34]. By contrast, they are consistent with the idea that reliable representations require an overall reduction of neural activity—potentially due to some mechanism of active inhibition [45]—or local desynchronization that increases entropy and thus improves information capacity [46, 47]. Indeed, several previous iEEG studies showed that at least in the low gamma band (~40-Hz) power reductions rather than increases are beneficial for memory processes [15, 16]. Furthermore, repeated presentations of real-world stimuli are associated with significant reductions of GBA in visual association cortex [48, 49]. This process was interpreted as a “sharpening” of representations and may be an important mechanism during the formation of novel memory traces [45, 50, 51]. In line with this interpretation, we found that overall levels of GBA were higher during unsuccessful than successful retrieval trials, indicating that reductions of GBA are indeed functionally relevant.

Although we used a spatial navigation paradigm, in our analyses we compared representations during viewing of the same sequence compared to during viewing of different sequences. Therefore, both conditions were characterized by the same degree of visual motion and engagement in spatial navigation. On the other hand, it is possible that representational similarity between encoding and retrieval is partly due to perception of the same stimuli. There are previous studies indicating a role of GBA for representing specific information in sensory cortex [52], including visual [53] and auditory cortex [54]. We conducted several control analyses and one control experiment to dissociate the memory-related RSA effect from perception-related RSA effects (Supplemental Information 3.3 and 3.4). Although we cannot completely rule out that the similarity of perceptual representations partly explains our results, these results suggest that representational similarity is indeed related to successful retrieval. Future studies are needed to address on this question in greater detail.

#### Supplemental Information

Supplemental Information includes Supplemental Experimental Procedures, Supplemental Results, Supplemental Discussion, four figures, and two movies and can be found with this article online at <http://dx.doi.org/10.1016/j.cub.2015.01.011>.

#### Author Contributions

H.Z., J.F., B.P.S., and N.A. designed the experiment. B.W. provided experiment materials. B.P.S. conducted the experiment. C.E.E. recruited and prepared patients. H.Z. analyzed the data. H.Z., J.F., and N.A. wrote the paper.

#### Acknowledgments

H.Z. and N.A. were supported by grant AX82/2 from the German Research Foundation. N.A. and J.F. received additional funding through the SFB 1089. B.P.S. is funded by a Sir Henry Wellcome Postdoctoral Fellowship.

B.W. is supported by Heisenberg grant WE 4427/3-1. We thank Arne Ekstrom and Andrew Watrous for helpful comments on the manuscript and Leila Chaieb and Thomas Reber for help in data collection of the control experiment.

Received: September 11, 2014

Revised: December 9, 2014

Accepted: January 5, 2015

Published: February 12, 2015

#### References

1. Abeles, M. (1982). *Local Cortical Circuits: An Electrophysiological Study* (Springer).
2. Palm, G. (1990). Cell assemblies as a guideline for brain research. *Concepts Neurosci.* 7, 133–148.
3. Cohen, N.J., and Eichenbaum, H. (1993). *Memory, Amnesia, and the Hippocampal System* (MIT Press).
4. Waydo, S., Kraskov, A., Quiñero, R., Fried, I., and Koch, C. (2006). Sparse representation in the human medial temporal lobe. *J. Neurosci.* 26, 10232–10234.
5. Buzsáki, G. (2006). *Rhythms of the Brain* (Oxford University Press).
6. Singer, W., and Gray, C.M. (1995). Visual feature integration and the temporal correlation hypothesis. *Annu. Rev. Neurosci.* 18, 555–586.
7. Singer, W. (1999). Neuronal synchrony: a versatile code for the definition of relations? *Neuron* 24, 49–65, 111–125.
8. Fries, P. (2009). The model- and the data-gamma. *Neuron* 64, 601–602.
9. Canolty, R.T., Ganguly, K., Kennerley, S.W., Cadieu, C.F., Koepsell, K., Wallis, J.D., and Carmena, J.M. (2010). Oscillatory phase coupling coordinates anatomically dispersed functional cell assemblies. *Proc. Natl. Acad. Sci. USA* 107, 17356–17361.
10. Jutras, M.J., and Buffalo, E.A. (2010). Synchronous neural activity and memory formation. *Curr. Opin. Neurobiol.* 20, 150–155.
11. Fell, J., and Axmacher, N. (2011). The role of phase synchronization in memory processes. *Nat. Rev. Neurosci.* 12, 105–118.
12. Jacobs, J., and Kahana, M.J. (2009). Neural representations of individual stimuli in humans revealed by gamma-band electrocorticographic activity. *J. Neurosci.* 29, 10203–10214.
13. Manning, J.R., Polyn, S.M., Baltuch, G.H., Litt, B., and Kahana, M.J. (2011). Oscillatory patterns in temporal lobe reveal context reinstatement during memory search. *Proc. Natl. Acad. Sci. USA* 108, 12893–12897.
14. van Gerven, M.A., Maris, E., Sperling, M., Sharan, A., Litt, B., Anderson, C., Baltuch, G., and Jacobs, J. (2013). Decoding the memorization of individual stimuli with direct human brain recordings. *Neuroimage* 70, 223–232.
15. Sederberg, P.B., Schulze-Bonhage, A., Madsen, J.R., Bromfield, E.B., McCarthy, D.C., Brandt, A., Tully, M.S., and Kahana, M.J. (2007). Hippocampal and neocortical gamma oscillations predict memory formation in humans. *Cereb. Cortex* 17, 1190–1196.
16. Fell, J., Klaver, P., Lehnertz, K., Grunwald, T., Schaller, C., Elger, C.E., and Fernández, G. (2001). Human memory formation is accompanied by rhinal-hippocampal coupling and decoupling. *Nat. Neurosci.* 4, 1259–1264.
17. Kriegeskorte, N., Mur, M., and Bandettini, P. (2008). Representational similarity analysis - connecting the branches of systems neuroscience. *Front. Syst. Neurosci.* 2, 4.
18. Tulving, E. (1972). Organization of memory. In *Episodic and Semantic Memory*, E. Tulving and W. Donaldson, eds. (Academic Press), pp. 381–402.
19. Rissman, J., and Wagner, A.D. (2012). Distributed representations in memory: insights from functional brain imaging. *Annu. Rev. Psychol.* 63, 101–128.
20. Polyn, S.M., Natu, V.S., Cohen, J.D., and Norman, K.A. (2005). Category-specific cortical activity precedes retrieval during memory search. *Science* 310, 1963–1966.
21. Kuhl, B.A., Rissman, J., Chun, M.M., and Wagner, A.D. (2011). Fidelity of neural reactivation reveals competition between memories. *Proc. Natl. Acad. Sci. USA* 108, 5903–5908.
22. Staresina, B.P., Henson, R.N., Kriegeskorte, N., and Alink, A. (2012). Episodic reinstatement in the medial temporal lobe. *J. Neurosci.* 32, 18150–18156.
23. Gordon, A.M., Rissman, J., Kiani, R., and Wagner, A.D. (2014). Cortical reinstatement mediates the relationship between content-specific encoding activity and subsequent recollection decisions. *Cereb. Cortex* 24, 3350–3364.

24. Ritchey, M., Wing, E.A., LaBar, K.S., and Cabeza, R. (2013). Neural similarity between encoding and retrieval is related to memory via hippocampal interactions. *Cereb. Cortex* *23*, 2818–2828.
25. Gelbard-Sagiv, H., Mukamel, R., Harel, M., Malach, R., and Fried, I. (2008). Internally generated reactivation of single neurons in human hippocampus during free recall. *Science* *322*, 96–101.
26. Buchsbaum, B.R., Lemire-Rodger, S., Fang, C., and Abdi, H. (2012). The neural basis of vivid memory is patterned on perception. *J. Cogn. Neurosci.* *24*, 1867–1883.
27. Ramot, M., Fisch, L., Davidesco, I., Harel, M., Kipervasser, S., Andelman, F., Neufeld, M.Y., Kramer, U., Fried, I., and Malach, R. (2013). Emergence of sensory patterns during sleep highlights differential dynamics of REM and non-REM sleep stages. *J. Neurosci.* *33*, 14715–14728.
28. Iaria, G., Fox, C.J., and Barton, J.J.S. (2013). Dynamic versus static stimuli for localization of the cerebral areas involved in face perception. *J. Vis.* *8*, 406–406.
29. Luo, H., and Poeppel, D. (2007). Phase patterns of neuronal responses reliably discriminate speech in human auditory cortex. *Neuron* *54*, 1001–1010.
30. Hasson, U., Nir, Y., Levy, I., Fuhrmann, G., and Malach, R. (2004). Intersubject synchronization of cortical activity during natural vision. *Science* *303*, 1634–1640.
31. Kumar, S., Bonnici, H.M., Teki, S., Agus, T.R., Pressnitzer, D., Maguire, E.A., and Griffiths, T.D. (2014). Representations of specific acoustic patterns in the auditory cortex and hippocampus. *Proc. Biol. Sci.* *281*, 20141000.
32. Bullock, T.H., McClune, M.C., Achimowicz, J.Z., Iragui-Madoz, V.J., Duckrow, R.B., and Spencer, S.S. (1995). EEG coherence has structure in the millimeter domain: subdural and hippocampal recordings from epileptic patients. *Electroencephalogr. Clin. Neurophysiol.* *95*, 161–177.
33. Menon, V., Freeman, W.J., Cuttillo, B.A., Desmond, J.E., Ward, M.F., Bressler, S.L., Laxer, K.D., Barbaro, N., and Gevins, A.S. (1996). Spatio-temporal correlations in human gamma band electrocorticograms. *Electroencephalogr. Clin. Neurophysiol.* *98*, 89–102.
34. Eckhorn, R., Bauer, R., Jordan, W., Brosch, M., Kruse, W., Munk, M., and Reitboeck, H.J. (1988). Coherent oscillations: a mechanism of feature linking in the visual cortex? Multiple electrode and correlation analyses in the cat. *Biol. Cybern.* *60*, 121–130.
35. Gray, C.M., König, P., Engel, A.K., and Singer, W. (1989). Oscillatory responses in cat visual cortex exhibit inter-columnar synchronization which reflects global stimulus properties. *Nature* *338*, 334–337.
36. Tallon-Baudry, C., and Bertrand, O. (1999). Oscillatory gamma activity in humans and its role in object representation. *Trends Cogn. Sci.* *3*, 151–162.
37. Sohal, V.S., Zhang, F., Yizhar, O., and Deisseroth, K. (2009). Parvalbumin neurons and gamma rhythms enhance cortical circuit performance. *Nature* *459*, 698–702.
38. Oehr, C.R., Hanslmayr, S., Fell, J., Deuker, L., Kremers, N.A., Do Lam, A.T., Elger, C.E., and Axmacher, N. (2014). Neural communication patterns underlying conflict detection, resolution, and adaptation. *J. Neurosci.* *34*, 10438–10452.
39. Manning, J.R., Jacobs, J., Fried, I., and Kahana, M.J. (2009). Broadband shifts in local field potential power spectra are correlated with single-neuron spiking in humans. *J. Neurosci.* *29*, 13613–13620.
40. Miller, K.J., Sorensen, L.B., Ojemann, J.G., and den Nijs, M. (2009). Power-law scaling in the brain surface electric potential. *PLoS Comput. Biol.* *5*, e1000609.
41. Burke, J.F., Zaghoul, K.A., Jacobs, J., Williams, R.B., Sperling, M.R., Sharan, A.D., and Kahana, M.J. (2013). Synchronous and asynchronous theta and gamma activity during episodic memory formation. *J. Neurosci.* *33*, 292–304.
42. Buzsáki, G., and Wang, X.J. (2012). Mechanisms of gamma oscillations. *Annu. Rev. Neurosci.* *35*, 203–225.
43. König, P., Engel, A.K., and Singer, W. (1996). Integrator or coincidence detector? The role of the cortical neuron revisited. *Trends Neurosci.* *19*, 130–137.
44. Fries, P. (2005). A mechanism for cognitive dynamics: neuronal communication through neuronal coherence. *Trends Cogn. Sci.* *9*, 474–480.
45. Axmacher, N., Elger, C.E., and Fell, J. (2008). Memory formation by refinement of neural representations: the inhibition hypothesis. *Behav. Brain Res.* *189*, 1–8.
46. Salinas, E., and Sejnowski, T.J. (2000). Impact of correlated synaptic input on output firing rate and variability in simple neuronal models. *J. Neurosci.* *20*, 6193–6209.
47. Hanslmayr, S., Staudigl, T., and Fellner, M.C. (2012). Oscillatory power decreases and long-term memory: the information via desynchronization hypothesis. *Front. Hum. Neurosci.* *6*, 74.
48. Gruber, T., and Müller, M.M. (2002). Effects of picture repetition on induced gamma band responses, evoked potentials, and phase synchrony in the human EEG. *Brain Res. Cogn. Brain Res.* *13*, 377–392.
49. Gruber, T., and Müller, M.M. (2005). Oscillatory brain activity dissociates between associative stimulus content in a repetition priming task in the human EEG. *Cereb. Cortex* *15*, 109–116.
50. Ranganath, C., and Ritchey, M. (2012). Two cortical systems for memory-guided behaviour. *Nat. Rev. Neurosci.* *13*, 713–726.
51. Park, H., Lee, D.S., Kang, E., Hahn, J., Kim, J.S., Chung, C.K., and Jensen, O. (2014). Blocking of irrelevant memories by posterior alpha activity boosts memory encoding. *Hum. Brain Mapp.* *35*, 3972–3987.
52. Sedley, W., and Cunningham, M.O. (2013). Do cortical gamma oscillations promote or suppress perception? An under-asked question with an over-assumed answer. *Front. Hum. Neurosci.* *7*, 595.
53. Ray, S., and Maunsell, J.H. (2011). Different origins of gamma rhythm and high-gamma activity in macaque visual cortex. *PLoS Biol.* *9*, e1000610.
54. Sedley, W., Teki, S., Kumar, S., Overath, T., Barnes, G.R., and Griffiths, T.D. (2012). Gamma band pitch responses in human auditory cortex measured with magnetoencephalography. *Neuroimage* *59*, 1904–1911.